JURNAL UPI

Indonesian Journal of Science & Technology

Journal homepage: http://ejournal.upi.edu/index.php/ijost/

IJoST Indonesian Journal of Science & Technology

Failure Investigation of Plastic Shredding Machine's Flange Coupling Based on Mechanical Analysis

Ignatius Pulung Nurprasetio[1], Bentang Arief Budiman[1,2], Farid Triawan[3]*

[1] Faculty of Mechanical and Aerospace Engineering, Institut Teknologi Bandung, Ganesha no. 10, Bandung 40132, Indonesia

[2] National Center for Sustainable Transportation Technology, Ganesha no. 10, Bandung 40132, Indonesia

[3] Department of Transdisciplinary Science and Engineering, Tokyo Institute of Technology, 2-12-1, Ookayama, Meguro-ku, Tokyo 152-8552, Tokyo, Japan

* Correspondence : E-mail: ipn@ftmd.itb.ac.id

ABSTRACT

This paper presented the investigation of failure mechanism of plastic shredding machine's flange coupling which is made of cast steel. The machine unexpectedly stalled a few minutes after High-Density Polyethylene (HDPE) plastic bottles were fed into the machine. It was discovered afterward that the flange broke with the large crack surface. Finite element analysis (FEA) was performed to find the position and value of the critical stresses in the flange during operating condition. Subsequently, hardness test was conducted on the flange body to determine the Brinell hardness which was then converted into the approximate ultimate tensile strength (σ_u). As a result, a maximum Von Mises stress of 287 MPa was confirmed from the FEA to be concentrated in the flange's keyway. Although this was found to be lower than the approximate σ_u obtained from hardness testing i.e. 449 MPa, the critical stress indicated an unstable condition which may induce a crack initiation any time when vibration or dynamic load occurs. Based on these analyses, it was concluded that the failure had been initiated by dynamic rather than static loading generated during machine stall condition. The dynamic load caused crack initiation at a stress concentration point of the keyway. The crack then propagated rapidly, breaking the flange body.

ARTICLE INFO

Article History:
Submitted/Received 14 Feb 2017
First Revised 01 May 2017
Accepted 29 Aug 2017
First Available online 30 Aug 2017
Publication Date 01 Sep 2017

Keyword:
Failure analysis,
Keyway,
Fixed flange coupling,
Finite element analysis,
Hardness testing,
Plastic shredding machine.

1. INTRODUCTION

Plastic shredding machine is an important machinery for waste recycling process (Alsalem, 2009). The machine is positioned in the first stage of recycling process in order to reduce the storage volume of plastic waste especially for plastic bottles and to simplify the washing process. **Figure 1** shows the plastic waste before and after the shredding. Volume-reduction up to 5 (five) times is achieved upon shredding by the machine. This reduction could increase the efficiency of the waste storage which eventually would significantly reduce the total processing cost of plastic waste recycling (Pace *et al.*, 2003).

Plastic shredding machine is usually designed with zero maintenance, meaning that it is not supposed to be repaired until the end of service except for the blade sharpening and replacement (Bugli and Green, 2005). This is because the price of the shredding machine should be economical. Thus, purchasing a new plastic shredding machine is considered more efficient than repairing an old one. The only part that might need sharpening or replacement is the blade. Moreover, the blade which is usually made of steel can be hardened for increasing its service life by quenching process which should also consider a corrosion risk in the process (Kurniawan, 2016). However, it is often difficult to find the spare part due to the special design and also the zero maintenance assumption. In addition, the failure of plastic shredding machine's components during operation might cause termination of the recycling process, which in turn would decrease the potential profit. For these reasons, a plastic shredding machine should be designed to have a good reliability and long service lifetime.

Our mechanical design group has successfully designed a small-scale portable shredding machine with the capacity to shred plastic waste up to 20 kg/hour as requested by our partner. The machine was manufactured using available components in the market. However, it was reported that during the trial period, the machine suddenly stopped during operation just within few minutes after several High-Density Polyethylene (HDPE) plastic bottles were fed into the cutting section. After a preliminary investigation, one flange coupling of the machine was found to be broken, cutting off the load transfer from the electric motor to the shredding cutter. To prevent the incident and increase the reliability of the prototype, we need to understand the failure mechanism of the broken flange coupling.

Figure 1. Plastic waste before (a) and after shredding (b) (Courtesy of CV Peka, Jl. Sapan Raya 1A, Bojongsoang, Bandung).

DOI: http://dx.doi.org/10.17509/ijost.v2i2
p- ISSN 2528-1410 e- ISSN 2527-8045

In this paper, analysis of failure mechanism of the broken flange coupling is presented. Finite Element Analysis (FEA) is initially performed in order to evaluate the stress condition during operation. Meshing process of the FEA model is carefully executed to obtain a reasonable FEA result. Following the FEA, the ultimate tensile strength (σ_u) of coupling material is estimated by performing hardness testing and converting the Brinell scale to tensile strength. The results from FEA and tensile strength are then compared and analyzed. Finally, failure mechanism of the broken flange coupling is comprehensively discussed

2. MATERIALS AND METHODS

2.1 Mechanism of Plastic Shredding Machine and Its Failure

Figure 2a shows a schematic figure of the plastic shredding machine. A 1.5 kW electric motor with a nominal speed of 1400 rpm is used to generate torque. A gear speed reducer with a transmission ratio of 1:10 is deployed before the driving shaft is connected to a flange coupling. The actual pictures of broken flange coupling and its fracture surface are shown in **Figure 2b**.

Figure 3 shows the detailed assembly sketch of the coupling consisting of the flanges, bolts, nuts, cylindrical bars, rings, and rubber surrounding the bolts. After some plastic wastes were put into the hopper, it will be shredded by a cutter made of hardened steel. This cutting process could generate a dynamic loading condition. In overload condition due to excessive input, the wastes might stuck inside the cutter, causing the machine to stop working. When this condition occurs, the flange coupling would have to bear the maximum torque generated by the motor.

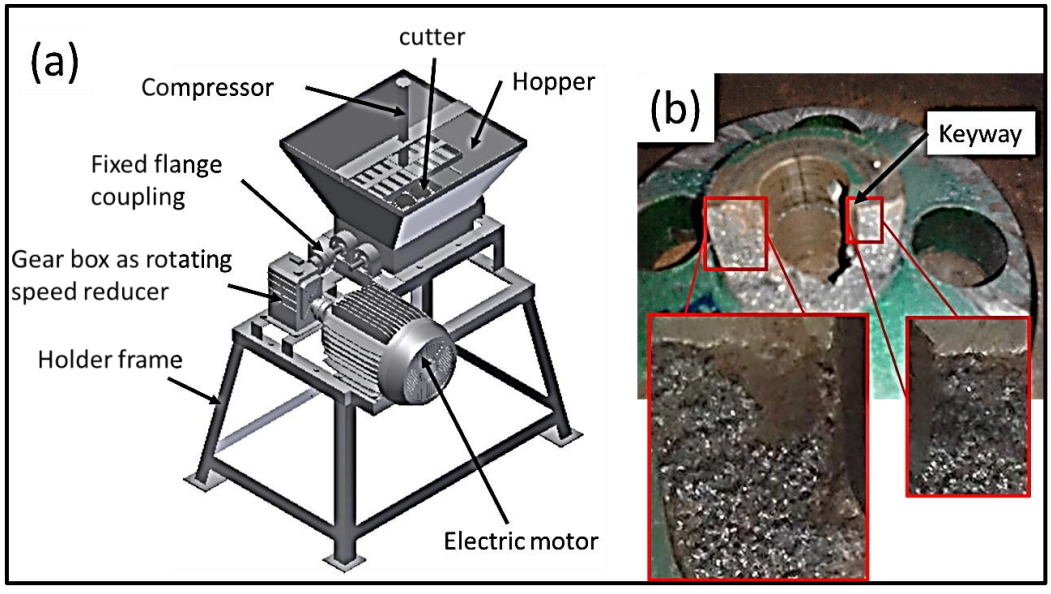

Figure 2. Schematic figure of plastic shredding machine (a) and its broken coupling (b).

DOI: http://dx.doi.org/10.17509/ijost.v2i2
p- ISSN 2528-1410 e- ISSN 2527-8045

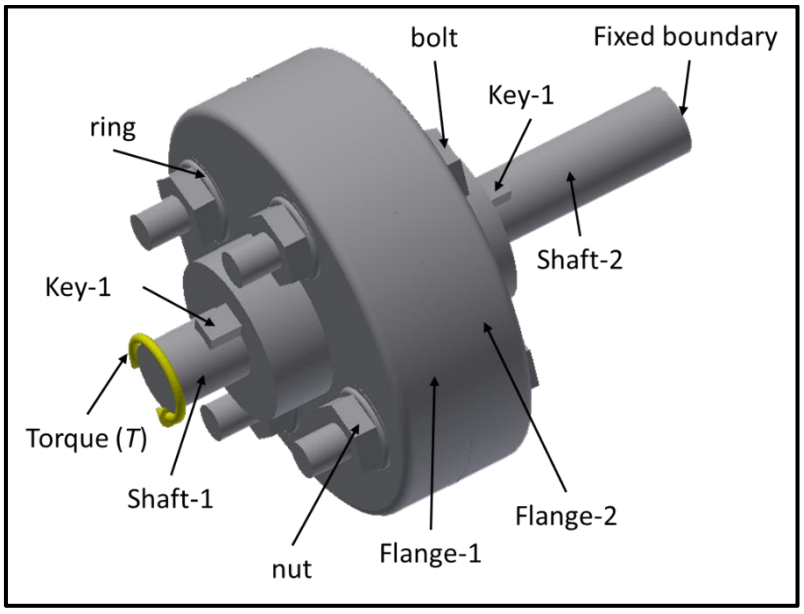

Figure 3. Modelling of couplings and other components.

According to the report during the trial period in the laboratory, the shredding machine suddenly stalled just 5 (five) minutes after some HDPE plastic bottles entered the cutting section. Specifically, flange-2 was found to be broken as shown in **Figure 2b**. Based on the visual observation, the broken surface indicated that the failure might be caused by a crack initiation near the keyway, then propagated rapidly until finally the flange body tear apart. A granular crack surface was observed, indicating the flange experienced a brittle failure which is the typical failure of cast steel (Batdorf, 1975). In fact, similar keyway failure has been reported by many researchers such as keyway failure in bridge crane shaft (Zambrano, *et al.*, 2014), high-speed shaft of pump (Li, *et al.*, 2016; Berndt, *et al.*, 2001), and elevator drive shaft (Göksenli, et al., 2009).

Keyway failure was not expected because the coupling material was carefully selected so that it could hold the maximum loading generated during stalled condition. In stalled condition, the machine experienced overload. For this, a fail-safe mechanism by sacrificing the flange bolts to protect the flanges is typical in coupling design technique (Budiman, *et al.*, 2016). This is because the cost to replace the bolts is much cheaper than the flanges. Furthermore, this will also reduce the downtime as compared to replacing the flanges. However, in this case, the flange was broken prior to the bolts. In order to clarify the failure mechanism, stress analysis of coupling structure under overload condition was conducted by FEA.

2.2 Finite Element Analysis

The finite element model was made by 3D CAD software SolidWorks 2016. First, it was redrawn following the actual geometry of the broken coupling as described in **Figure 3.** Then, FEA of the model was performed using the integrated tools provided in SolidWorks 2016. The contact surfaces connecting to the flanges were defined as 'no penetration' contact, thus neglecting friction. Other contact surfaces were defined as tie-contact in which separation and penetration were prohibited.

DOI: http://dx.doi.org/10.17509/ijost.v2i2
p- ISSN 2528-1410 e- ISSN 2527-8045

The boundary condition of shaft-2 was fixed (no rotation allowed), while a torque moment (*T*) was applied to shaft-1. The torsional loading from the torque was transferred from shaft-1 to flange-1 via key-1. Then, the load was transferred to flange-2 via the bolts. Finally, the load from flange-2 via key-2 was received by shaft-2, but, it was not allowed to rotate due to the fixed boundary condition.

The torque as the input data of FEA was calculated based on the available power of the electric motor. In this case, the relation as depicted in Equation 1 was used for the calculation.

$$P = T\omega \quad (1)$$

In the above equation, *P* is the power in W, *T* is torque in Nm, and ω is the angular velocity in rad/s. In this case, the power of electric motor (*P*) was 1500 W and ω was (2π x 140/60) rad/s. As a result, *T* of 102.4 Nm was obtained.

A linear elastic material without failure criterion is applied to the model. The flange material was cast steel with elastic modulus and Poisson`s ratio of 210 GPa and 0.3, respectively. This setting is appropriate because the purpose of the FEA was just to find the location and value of the critical stress. Furthermore, since the FEA was focused on analyzing the stress condition of the flange body, the other coupling components were considered as the rigid body so that they may be excluded from the stress analysis.

After the torque and boundary conditions were properly defined, meshing process was then conducted. Selection of the meshing element size should be conducted carefully in order to make sure the stress obtained from FEA represents the real condition. A coarse mesh might produce an irrelevant FEA result and far from reality. In contrast, a fine mesh will give an accurate result but may consume a long time. Thus, the meshing element size should be selected by considering both conditions. In this work, four kinds of meshing element sizes were applied in the FEA model with four nodes forming tetrahedron.

In order to investigate whether the flange was broken due to static or dynamic loading, hardness testing was carried out to estimate the σ_u of the flange material. The value will be compared with the critical stress obtained from the FEA.

2.3 Material Testing

Brinell hardness indentation test was conducted in order to evaluate the σ_u of the flange material as shown in **Figure 4(a)** (ISO 6506-1, 2014). The flange surface is firstly polished by sandpaper to obtain a good accuracy of the test. The compressive force (*F*) imposed to the specimen was 3 kN with the diameter of ball indenter (*D*) was 10 mm. The indentation test was conducted at more than 5 different locations on the surface because each indentation only represents localized hardness of the material. The measured Brinell hardness numbers (*HB*) were then averaged. After the test, the diameter (*d*) of the indentation circle was measured with the aid of microscope as shown in **Figure 4(b)**.

HB was calculated by Equation 2 as:

$$HB = \frac{2F}{\pi D\left(D - \sqrt{D^2 - d^2}\right)} \quad (2)$$

The *HB* values are then converted to σ_u by using Equation 3 as follows (Gaško, 2011; E.J. Pavlina, 2008),

$$\sigma_u = \begin{cases} 3.55HB & (for\ HB \leq 175) \\ 3.38HB & (for\ HB > 175) \end{cases} \quad (3)$$

DOI: http://dx.doi.org/10.17509/ijost.v2i2
p- ISSN 2528-1410 e- ISSN 2527-8045

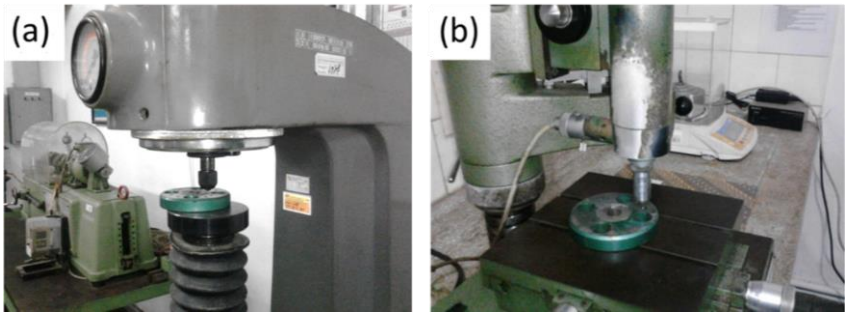

Figure 4. Indentation tests for broken coupling (a) and diameter measurement (b)

3. RESULTS AND DISCUSSION

Figure 5 shows the coupling's flanges with four different mesh size and its corresponding FEA results. **Figure 5(a)** shows the result from the coarsest meshing element size, whereas **Figure 5(d)** shows the result from the finest meshing element size. Other components such as shafts, bolts, and keys are excluded from the **Figure**. It can be seen that regardless of the meshing element size, the model exhibited a relatively low-stress value of between 0 and 150 MPa in most parts of its body. However, a critical stress was observed at the keyway area. This very high-stress concentration might be generated because of the sharp corner of the keyway.

Figures 5(a), **5(b)**, **5(c)**, and **5(d)** gives different values of maximum Von Mises stress at the same point on the keyway of flange-2. This fact matches the actual crack position of the broken flange shown in **Figure 2b**. For the coarsest meshed model shown in **Figure 5(a)**, the value of the maximum Von Mises stress is 157 MPa. The maximum stress value with meshing element size of 2 mm is 150 MPa, which does not change much as shown in **Figure 5(b)**. However, for the model with smaller meshing element size, shown in **Figure 5(c),** and **5(d),** the value of the maximum Von Mises stress got higher, such as 198 MPa for **Figure 5(c),** and 287 MPa for **Figure 5(d).** This result indicates that a stress singularity might have occurred in the sharp edge of the keyway. The presence of stress singularity could induce a crack propagation, especially for brittle material such as cast steel which might have impurities on the surface (Dahlberg, 1997). In addition, the results demonstrate that selection of mesh size is critical for FEA, since different mesh size may result in a different conclusion.

From the Brinnel hardness indentation tests, six locations were selected as shown in **Figure 6(a)**. Location-1, however, should be excluded from the analysis because the indenter contacted the edge of the flange-hub during the test. The results of *HB* values calculated from Equation 2 were then plotted as shown in **Figure 6(b)**. Furthermore, considering criterion expressed in Equation 3, an averaged σ_u value of 449 MPa was obtained. Comparing this value with the critical stress at the keyway shown in **Figure 5(d)**, it is confirmed that the stress concentration of 287 MPa was lower than the σ_u value but slightly higher than the endurance limit which may be calculated as half of σ_u or 224.5 MPa (Stephens, 2014). Hence, this high-stress value should not create static failure at the keyway. However, as the machine is operated, vibration occurs due to the dynamic load from the cutting action (Han, 2014). As a result, fluctuating load comes into play and produce relative motion between the key and its keyway. This might have aggravated the stress condition, especially at the stress concentration area, thus may have generated an unstable condition. Due to the above, a small crack

DOI: http://dx.doi.org/10.17509/ijost.v2i2
p- ISSN 2528-1410 e- ISSN 2527-8045

may initiate any time at the sharp corner of the keyway. Owing to the high-stress concentration, the small crack was then pushed to grow and propagate rapidly which eventually causing the brittle failure mode (low cycle fatigue) of the flange.

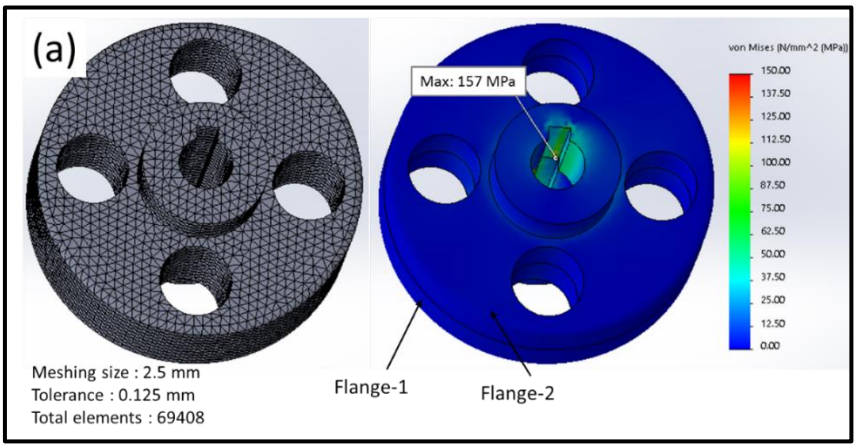

Figure 5a. Von Mises stress of the coupling's flanges with different mesh size of 2.5 mm

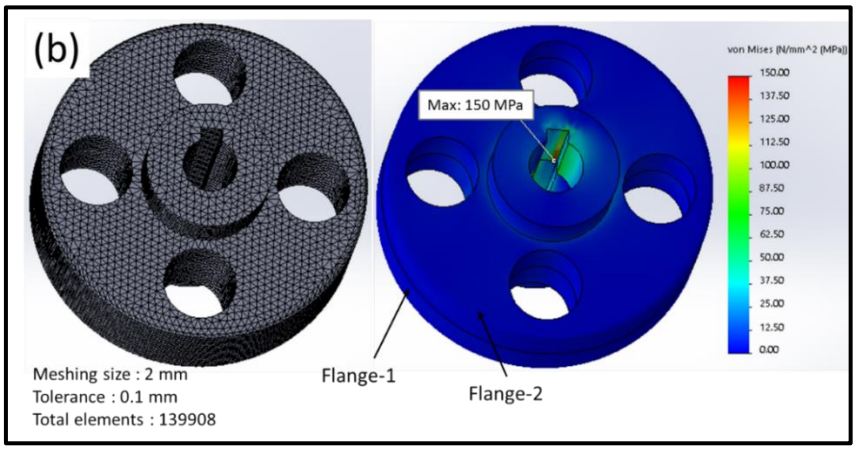

Figure 5b. Von Mises stress of the coupling's flanges with different mesh size of 2 mm

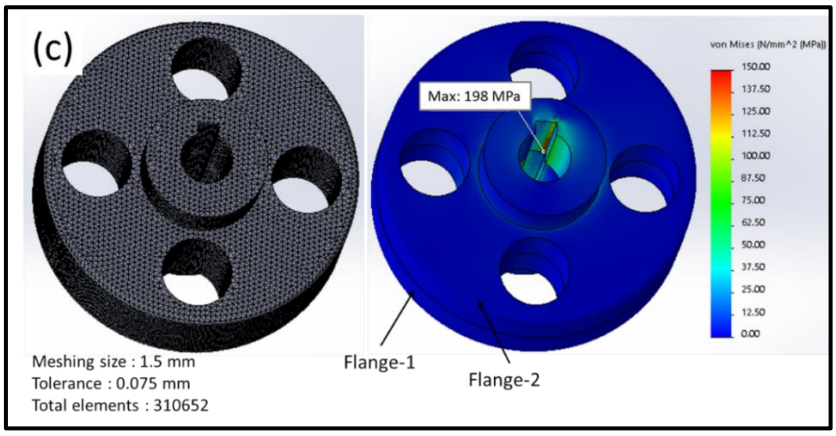

Figure 5c. Von Mises stress of the coupling's flanges with different mesh size of 1.5 mm

DOI: http://dx.doi.org/10.17509/ijost.v2i2
p- ISSN 2528-1410 e- ISSN 2527-8045

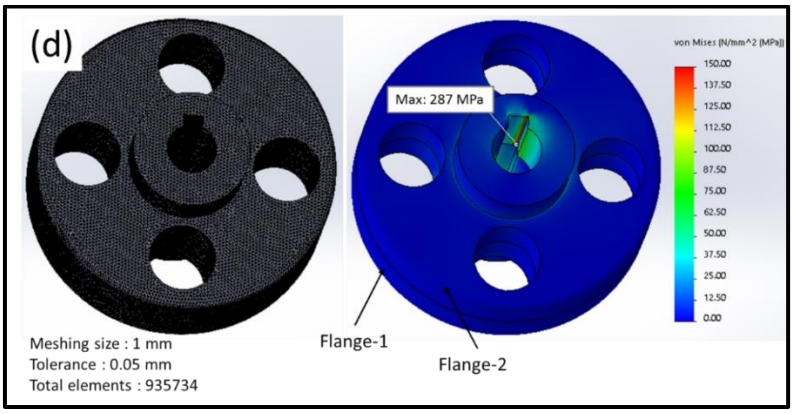

Figure 5d. Von Mises stress of the coupling's flanges with different mesh size of 1

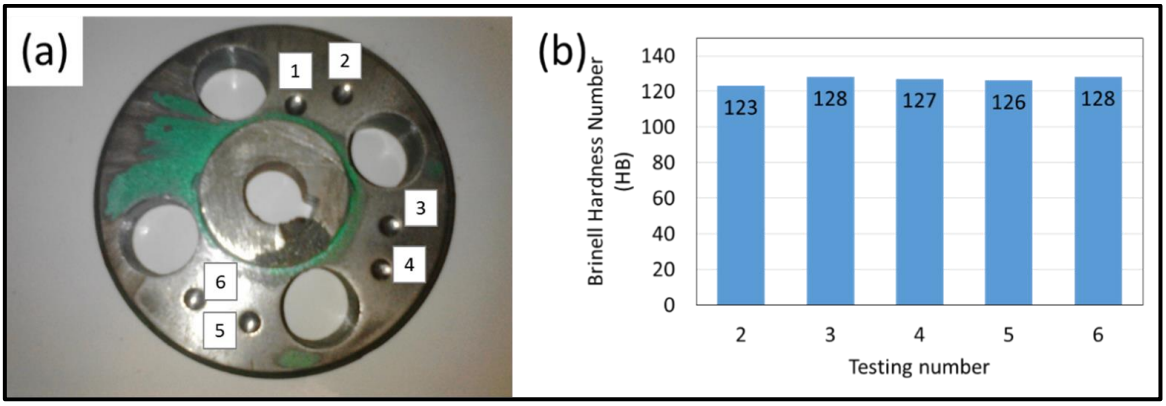

Figure 6. result of indentations (a) and Brinell Hardness Number (*HB*) (b)

Learning from the above, in order to improve the new flange, stress concentration at the keyway should be avoided by two approaches. The first approach is by changing the keyway geometry such as adding fillet in the corner (Pedersen, 2010; Orthwein, 1979). The fillet will redistribute the stress at the corner which in turn will reduce the stress concentration. However, this approach is not economical because of the relatively high machining cost. In the second approach, stress concentration may be avoided by selecting ductile materials such as middle-class low carbon steel. Even though the σ_u of the steel might be lower than the concentrated stress, the plastic deformation of the material may redistribute the stress and significantly reduce the stress concentration. In this case, the second approach was selected and implemented for the flange-2 coupling as shown in **Figure 7**. Following the modification, the machine operates properly as required by the design.

DOI: http://dx.doi.org/10.17509/ijost.v2i2
p- ISSN 2528-1410 e- ISSN 2527-8045

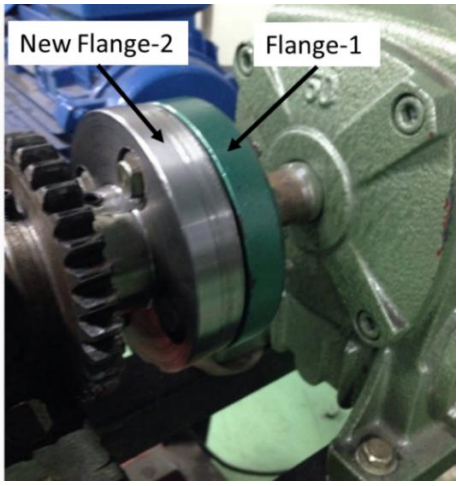

Figure 7. New flange-2 with material base of low carbon steel.

4. CONCLUSION

Investigation of failure mechanism of fixed flange coupling for transferring load in plastic shredding machine has been comprehensively discussed and analyzed. From the visual observation, a brittle failure had occurred in the flange coupling which was made of cast steel. From FEA with fine meshing, a critical stress of 287 MPa was revealed in a specific region near the keyway. This stress concentration indicated the origin of crack initiation. From hardness test, the approximate ultimate tensile strength of the coupling material was found to be 449 MPa. The endurance limit is thus 224.5 MPa. This value was in fact lower than the concentrated stress value obtained from FEA. This means that the failure was not caused by the static loading. Instead, it was initiated by the dynamic loading due to vibration during machine operation. The initial crack occurred in the concentrated stress point, then propagates due to the fluctuated dynamic load. Considering the brittle characteristic of the flange material, i.e., cast steel, the initiated crack propagates rapidly until the final failure.

5. ACKNOWLEDGEMENTS

The authors gratefully acknowledge the contribution of Theo Christianto and Kelvin in the prototyping stage, and to Rizky Ilhamsyah for his assist in drawing the 3-D model of the flange coupling.

6. AUTHORS' NOTE

The author(s) declare(s) that there is no conflict of interest regarding the publication of this article. Authors confirmed that the data and the paper are free of plagiarism.

7. REFERENCES

Alsalem, S. M. (2009). Recycling and recovery routes of plastic solid waste (PSW): A review. *Waste Management*, 29(10), 2625-2643.

Berndt, F., van Bennekom A. (2001). Pump shaft failures - a compendium of case studies. *Engineering Failure Analysis*, 8, 135-144

DOI: http://dx.doi.org/10.17509/ijost.v2i2
p- ISSN 2528-1410 e- ISSN 2527-8045

Batdorf, S. B. (1975). Fracture statistics of brittle materials with intergranular cracks. *Nuclear Engineering and Design*, 35(3), 349–360.

Budiman, B. A., Suharto, D., Djodikusumo, I., Aziz, M., Juangsa, F. B. (2016). Fail-safe design and analysis for the guide vane of a hydro turbine. *Advances in Mechanical Engineering*, 8(7), 1–8.

Bugli, N. and Green, G. (2005). Performance and Benefits of Zero Maintenance Air Induction Systems. *SAE Technical Paper*, doi:10.4271/2005-01-1139.

Dahlberg, M. (1997). Micromechanical modelling of nodular cast iron, a composite material. *International Journal of Cast Metals Research*, 9(6), 319-330.

Gaško, M. and Rosenberg G. (2011). Correlation between hardness and tensile properties in ultra-high strength dual phase steels. *Short communication Materials Engineering - Materiálové inžinierstvo*, 18, 155-159.

Göksenli, A., Eryürek I. B. (2009). Failure analysis of an elevator drive shaft. *Engineering Failure Analysis*, 16, 1011–1019.

Han, H. S. (2014). Analysis of Fatigue Failure on the Keyway of the Reduction Gear Input Shaft Connecting a Diesel Engine Caused by Tortional Vibration. *Engineering Failure Analysis*, 44, 285-298.

Kurniawan, T., Fauzi, F. A. B., and Asmara, Y. P. (2016). High-temperature Oxidation of Fe-Cr Steels in Steam Condition – A Review. *Indonesian Journal of Science & Technology*, 1 (1), 107 – 114.

Li, W., Xia, F., and Luo, B. (2016). Failure Analysis of a High-Speed Shaft Crack. *J Fail. Anal. and Preven*. DOI 10.1007/s11668-016-0172-4.

Orthwein, W. C. (1979). A New Key and Keyway Design. *Transactions of the ASME*, 101, 338 – 341.

Pace, G., Pisharody, S., and Fisher, J. (2003). Plastic Waste Processing and Volume Reduction for Resource Recovery and Storage in Space. *SAE Technical Paper* 2003-01-2369, doi: 10.4271/2003-01-2369.

Pavlina, E.J. and Van Tyne, C.J. (2008). Correlation of Yield Strength and Tensile Strength with Hardness for Steels. *Journal of Materials Engineering and Performance*, 17, 888–893.

Pedersen, N. L. (2010). Stress concentrations in keyways and optimization of keyway design. *The journal of strain analysis for engineering design*, 45, 593-604.

Stephens, R. I. (2001). Metal Fatigue in Engineering (2nd ed.). John Wiley & Sons, Inc. ISBN 0-471-51059-9.

STN EN ISO 6506-1 (2014). Metallic materials. Brinell hardness test. Part 1: Test method.

Zambrano, O. A., Coronado, J.J., Rodrı´guez, S.A. (2014). Failure analysis of a bridge crane shaft. *Case Studies in Engineering Failure Analysis*, 2, 25–32.

DOI: http://dx.doi.org/10.17509/ijost.v2i2
p- ISSN 2528-1410 e- ISSN 2527-8045